Elshewy *et al. Egypt J Radiol Nucl Med* (2024) 55:24
https://doi.org/10.1186/s43055-023-01181-z

Egyptian Journal of Radiology and Nuclear Medicine

RESEARCH

Open Access

# A proposed inclusion of magnetic resonance imaging features to the VI RADS to enhance its accuracy in predicting muscle invasion

Nesma Elshewy[1*], Adel Ali Ramadan[1], Wael Mohamed Sameh[2], Mohamed Emad-ElDeen Eid[1], Samar El Achy[3] and Omnia Ezz Eldin[1]

## Abstract

**Background** Muscle invasion in bladder cancer is a paramount factor in prognosis and setting the management plan. MRI is gaining preference in this field, being noninvasive with no radiation hazards and having good resolution, especially with the development of the standardized system of (VI RADS). Moreover, multiple other imaging features can aid in predicting muscle invasion. We studied some of the most commonly reported features to develop the most reliable combination to anticipate the presence of muscle invasion.

**Results** Our prospective study on 80 patients showed 39 (48.75%) muscle invasive (MIBC) and 41 (51.25%) non-muscle invasive (NMIBC) bladder cancer cases. The inter-observer agreement on the VI RADS score and the ADC measurements were very good and they had high-accuracy predicting muscle invasion with areas under the curve (AUCs) on ROC curve analysis reaching 0.905 and 0.857, respectively. The imaging variables that showed statistically significant differences between NMIBC and MIBC cases were: the multiplicity of the lesions, vesicoureteric junction (VUJ) involvement with distal ureteric backpressure, tumor–wall contact length (TCL), tumor volume, tumor shape (sessile or papillary), presence of a stalk, the final VI RADS score and the ADC value. On the multiple regression analysis model, the multiplicity of the lesions, the minimum ADC value by ROI method and the final VI RADS score showed independent correlation with muscle invasion, negatively with the first two and positively with the latter. The combination of the six statistically significant variables on the univariate regression analysis (final VI RADS score, minimum ADC by ROI, multiplicity, index tumor shape, TCL and distal ureteric backpressure changes) showed the best AUC (0.944).

**Conclusions** VI RADS has good diagnostic accuracy regarding muscle invasion; however, this can even be enhanced by including other quantitative and qualitative commonly reported MRI features as a proposed modification to the VI RADS.

**Keywords** Bladder cancer, Muscle invasion, VI RADS, MRI features

*Correspondence:
Nesma Elshewy
nesma.elsayed@alexmed.edu.eg; nessness.0107@gmail.com
[1] Diagnostic and Interventional Radiology Department, Alexandria Faculty of Medicine, 10 Shamplion Street, Alexandria 21131, Egypt
[2] Urology Department, Alexandria Faculty of Medicine, 10 Shamplion Street, Alexandria 21131, Egypt
[3] Pathology Department, Alexandria Faculty of Medicine, 10 Shamplion Street, Alexandria 21131, Egypt

## Background

Bladder cancer (BC) is the tenth most common cancer worldwide [1]. It is classified clinically as either non-muscle invasive (NMIBC) (70–80%) or muscle invasive (MIBC) (20–30%) with a widely divergent prognosis. Many factors including tumor grade and specific gene expressions impact the clinical course, yet the state of muscle invasion is dominant. Only 10–20% of the NMIBC progress to the invasive form while most

of them follow a course of repeated recurrences managed by local treatments and active surveillance. On the other hand, MIBC carries a much poorer prognosis, where occult or clinically detectable metastasis exists in 50% of the cases at the initial presentation warranting more aggressive treatment procedures [2, 3].

The multiparametric MR (mpMR) imaging of BC enables anatomical alongside functional evaluation. The high soft tissue contrast and the good resolution of the modern devices (especially the 3-T) [4] allow identifying the muscle layer and its interruption in most of MIBC. Moreover, the DW image reflects cellular density and the CE sequences reflect vascularity and perfusion patterns of the lesions improving the diagnostic capabilities of the MRI beyond the direct visualization to deep tissue characteristics [5].

Continuous advances in MR procedures and the development of the standardized reporting system of VI RADS even improved its validity, making it a preferable initially guiding imaging procedure, without radiation hazard before the definitive gold standard tissue diagnosis by transurethral resection of bladder tumor (TURBT) [6, 7]. Local staging of BC was the main application of the MRI, but current studies apply it to monitor response to neoadjuvant therapy with (nac VI RADS) and also for surveillance to detect disease recurrence [8, 9].

The VI RADS score includes structural category (SC) for the T2-weighted image, diffusion-weighted (DW) category and contrast-enhanced (CE) category, all assessing the integrity of the muscle layer considering tumor size and presence of stalk or thickened inner layer [10]. However, no quantitative variables exist within the current scoring system [11].

A quantitative marker for the biological behavior of tumors is the apparent diffusion coefficient (ADC) value derived from DW image [12, 13]. Variabilities in the utilized ADC value do exist with contradictions regarding the best-employed measurement also present [14, 15].

The ADC value together with other commonly reported quantitative and qualitative MR imaging features may represent a valuable add-on to the VI RADS score maximizing the utilization of the extracted data from the bladder cancer MR study to idealize the performance of the VI RADS score.

## Methods

### Study population

From January 2021 to January 2023, 150 patients presented to our Department of Radiodiagnosis for an MRI examination of a bladder mass. They underwent selection according to the flowchart in Fig. 1. Consequently, 80 patients were enrolled in the study and had no intervention within 2 weeks before the MR examination.

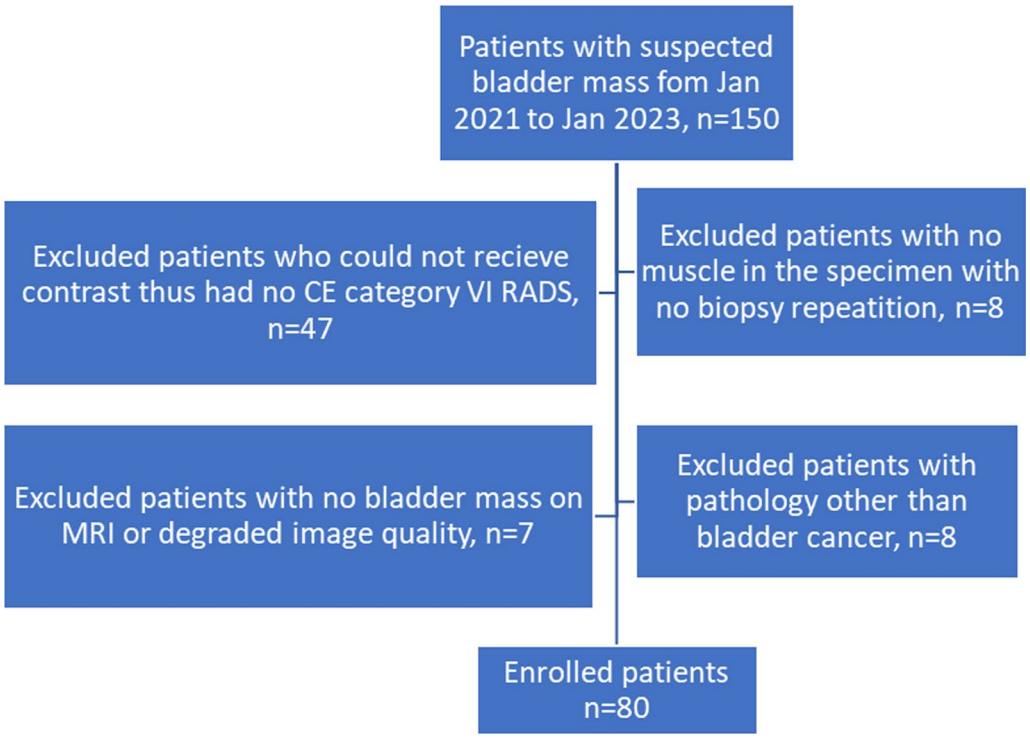


**Fig. 1** Flowchart for the selection procedure of the participants in the study

### MR imaging

For adequate bladder distension, patients were instructed to avoid urination for at least 1 h before the procedure. All examinations were performed on a 3.0-T MRI (Ingenia, PHILIPS MR systems, the Netherlands) applying a surface coil (16-channel torso phased array) covering the pelvic region in the supine position. The scanning protocol was in accordance with the authentic system of VI RADS published in 2018 [10].

### Image analysis

All the images were transferred to a workstation with a DICOM viewer (Osirix v.5.6 64-bit, Pixmeo Sarl, Switzerland). Two abdominal radiologists with more than 10 years of experience in urogenital MRI reporting analyzed the images independently being blinded to patients' clinical data, pathology reports and each other's results. A consensus was obtained for categorical variables, and averages were calculated for numeric ones.

For ADC, the mean and the minimum values were obtained by region of interest (ROI) and volumetric methods. To measure the mean ADC by the ROI method, the mean value of three circular ROIs placed within the most representative solid tumor areas was calculated. The minimum ADC by ROI was obtained by placing a small circular ROI (with an area in the range of 2–5 $mm^2$) at the visually determined prominently restricted areas. Volumetric mean and minimum ADC were automatically calculated by the DICOM viewer after manual segmentation of the lesions. In both methods the stalk, necrotic and hemorrhagic areas were excluded. Normalization of the values was not required in our study as all the examinations were performed by the same protocol on the same device.

In patients with multiple tumors, a representative index lesion was identified as the highest stage on an imaging basis or the largest one among lesions with similar radiological stages.

### Histopathologic analysis

All the patients underwent cystoscopic TURBT biopsies. Thirteen patients did not have muscularis propria on the initial TURBT, so it was repeated (re-TURBT) within 2–3 weeks later in 9 patients while the other 4 patients underwent upfront radical cystectomy being of high risk. Radical cystectomy was also done subsequently in other indicated patients. Staging was done according to the TNM classification of AJCC cancer staging manual 8th edition differentiating NMIBC (< T2) from MIBC (≥ T2).

### Statistical analysis

Statistical analyses were performed by using IBM SPSS software (v. 20.0, Armonk, NY: IBM Corp). The abnormally distributed continuous (quantitative) variables were compared by Mann–Whitney (*U*) test while categorical variables were compared by the Chi-square ($\chi^2$) test (applying Fisher's exact or Monte Carlo correction when needed) between MI and NMI cases.

The diagnostic performance of the VI RADS scores (SC, DW, CE and final) and the ADC values (mean and minimum by both ROI and volumetric methods) was determined by receiver operating characteristic (ROC) curve analysis choosing the cutoff value by the Youden index to calculate sensitivity, specificity, positive and negative predictive values.

All the radiological variables that proved to have a statistically significant difference between NMIBC and MIBC were included in univariable logistic regression analysis to evaluate their ability in predicting muscle invasion. Then, features that proved significant were further incorporated in a multivariable regression model to determine which variables can independently predict muscle invasion. The effect of combining other imaging features to the VI RADS score was evaluated by ROC curve analysis to determine the best combination of features achieving the highest AUC.

## Results

### Patients and tumors demographics

Our 80 patients included 73 males (91.3%) and 7 females (8.8%). Their median age was 64 years with interquartile range (IQR) between 56.5 and 70 years. TURBT was done in all patients and re-TURBT in 21 (26.25%) patients; 9 of them were due to the lack of muscularis propria, and radical cystectomy was performed in 19 (23.75%) patients. Multiple tumors were found in 45 patients (56.3%) where only one representative index lesion was analyzed. MIBC cases were 39 (48.75%), and NMIBC were 41 (51.25%). Examples of NMIBC and MIBC lesions are clarified in Figs. 2, 3, 4 and 5.

### Imaging variables showing statistically significant differences between NMIBC and MIBC cases (Tables 1 and 2)

Multiplicity of lesions was more common in NMI cases, being reported in three quarters of them compared to 35.9% of the MI cases.

The MI lesions were more likely to involve the VUJ causing distal ureteric backpressure changes (79.5% and 64.1%, respectively) compared to NMI lesions (56.1% and 26.8%, respectively).

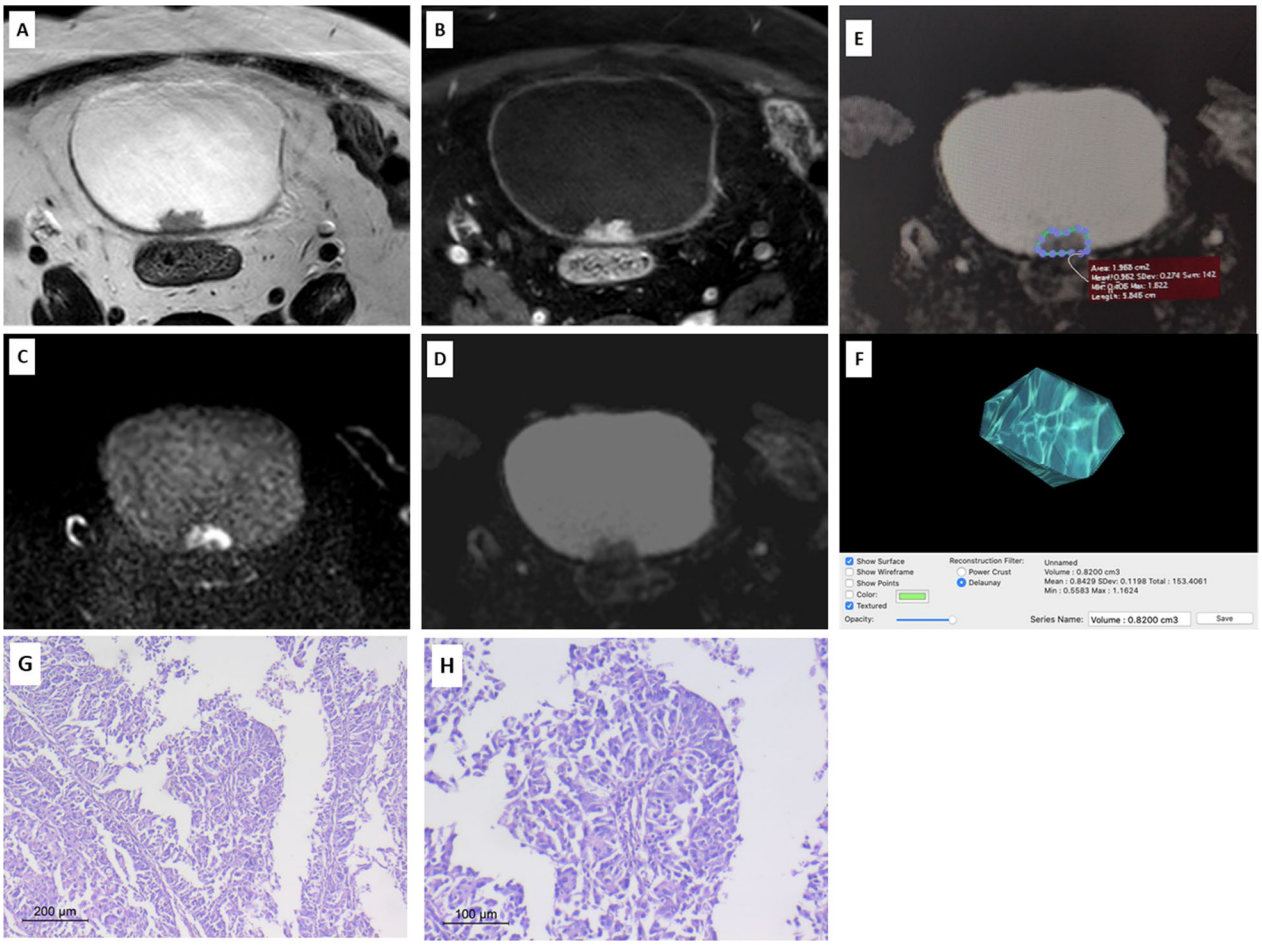


**Fig. 2** A high-grade NMIBC. It is a single papillary lesion with no stalk, TCL < 3 cm, 0.8 $cm^3$ in volume, no distal ureteric backpressure, the minimum ADC by selected ROI $0.65 \times 10^{-3}$ $mm^2/s$ and final VI RADS score of 3. **A** Axial T2WI FSE, **B** axial T1WI fat suppression post-contrast, **C** axial DWI at b-value 1000, **D** axial ADC map, **E** tumor segmentation at one slice, **F** calculation of the volumetric values. **G** Histopathological image showing high-grade papillary TCC (100X), **H** higher-power view (200X)

As regards the shape of the lesion, most of the NMI lesions were papillary (90.2%) in contrast to the MI lesions which were nearly equally distributed having 19 papillary and 20 sessile lesions.

The tumor–wall contact length (TCL) was categorized into ≤3 cm and >3 cm. The NMI lesions had a smaller TCL than the MI lesions where 61% of the NMI lesions had TCL ≤ 3 cm and only 12.8% of the MI cases were so. On the other hand, the tumor volume in $cm^3$ showed a larger mean value in MIBC (2.60 ± 1.33 $cm^3$) than in NMIBC (2.15 ± 1.22 $cm^3$).

The fibrovascular stalk was more commonly present in NMI cases (58.5%) and was seen in only 23.1% of the MI cases. The stalk was eccentric in all MI cases, but was equally distributed between central and eccentric appearance in the NMI cases.

Comparing different categories of the VI RADS scores between NMI and MI cases revealed that most of the NMI cases (80.5–82.9%) had a score of 3 or less in contrast to the MI cases which had a score > 3 in 89.7% of the cases, but only 4 MI cases had a score equal 3 in all categories and in the final score. The diagnostic performance of the VI RADS to predict muscle invasion with the optimum cutoff value at score 3 revealed that the DW score had the largest AUC (0.905) with 89.74%, 82.93%, 83.33% and 89.47% sensitivity, specificity, positive and negative predictive values, respectively.

Concerning the ADC values (mean and minimum) measured by both methods (ROI and volumetric), the averaged values in NMI were significantly higher than those for MI cases. On studying their validity, the AUCs ranged from 0.781 to 0.857 with the highest was for the minimum ADC value by the ROI method as illustrated in Table 3.

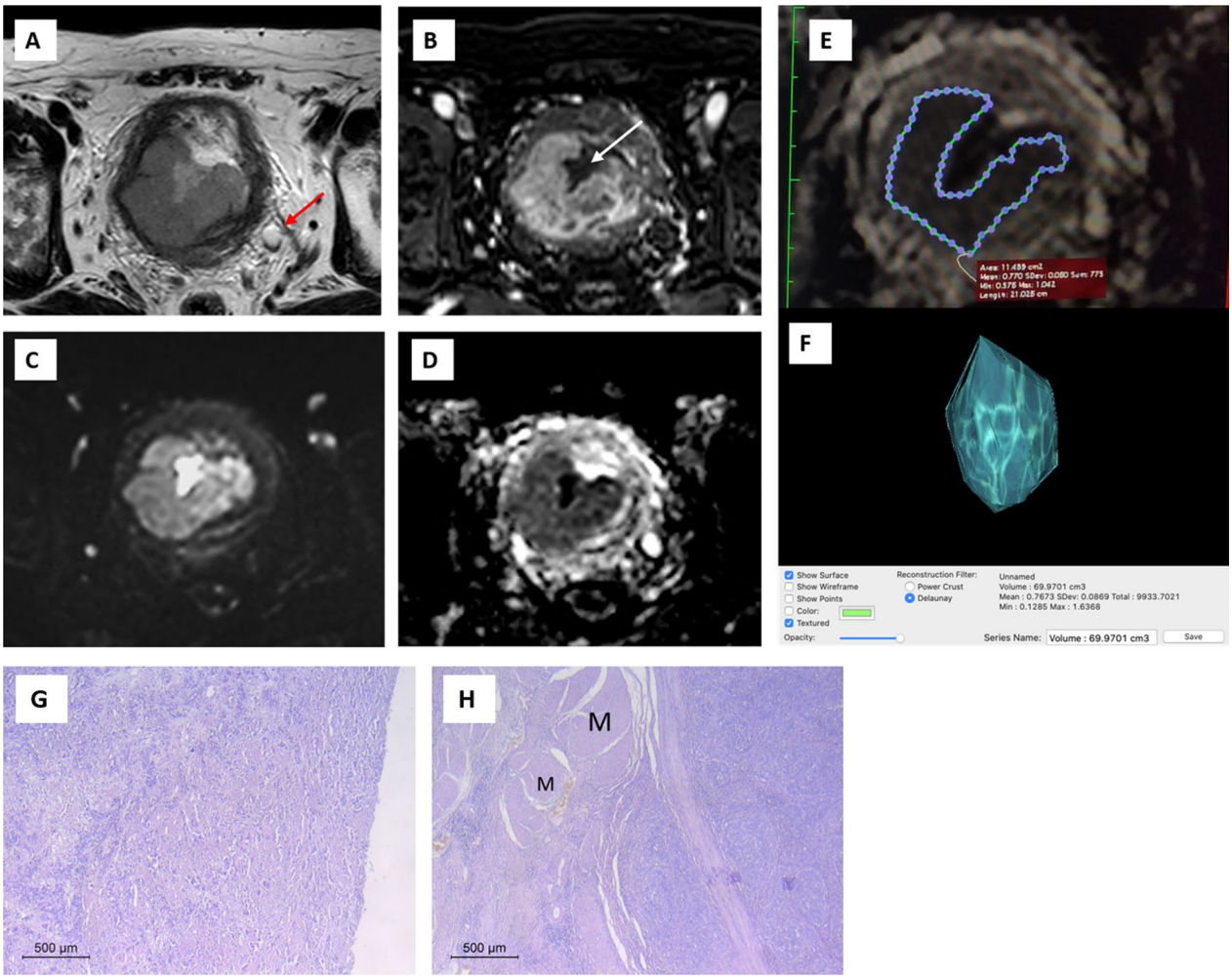


**Fig. 3** A high-grade MIBC. It is a single non-papillary lesion with no thickened inner layer, TCL > 3 cm, 70 $cm^3$ in volume, with distal ureteric backpressure, the minimum ADC by selected ROI $0.45 \times 10^{-3}$ $mm^2/s$ and the final VI RADS score 4. **A** Axial T2WI FSE with red arrow pointing to dilated distal left ureter, **B** axial T1WI fat suppression post-contrast with white arrow pointing to non-enhancing intravesical hematoma, **C** axial DWI at b-value 1000, **D** axial ADC map, **E** tumor segmentation at one slice, **F** calculation of the volumetric values. **G** Histopathological image showing high-grade urothelial carcinoma invading the lamina propria with ulceration of the surface (40X), **H** invasion of the muscularis propria (M) (40X)

### Imaging variables without statistically significant differences between NMIBC and MIBC cases (Table 4)

Different tumor locations except for vesicoureteric junction (VUJ), the tumoral urethral extension and the desmoplastic mural retraction were not significantly different between NMIBC and MIBC.

### Logistic regression analysis (Table 5)

The univariate analysis to predict muscle invasion included seven imaging variables that were multiplicity (multiple or single), distal ureteric backpressure changes (present or absent), the final VI RADS score in two categories (≤ 3 and > 3), index tumor TCL also in two categories (≤ 3 and > 3 cm) and tumor shape (sessile or papillary) as categorical variables while numeric variables were tumor volume and the minimum ADC value by ROI method being the one with the highest AUC in the ROC curve analysis. All correlated well with MIBC except the tumor volume ($p = 0.221$), so it was not subsequently included in the multivariate analysis. The variables showing independent correlation with the MIBC on the multivariate regression model were the final VI RADS score ($p = 0.030$), minimum ADC by ROI method ($p = 0.020$) and multiplicity of the lesions ($p = 0.024$) with positive correlation with the VI RADS score and negative with the minimum ADC and the multiplicity.

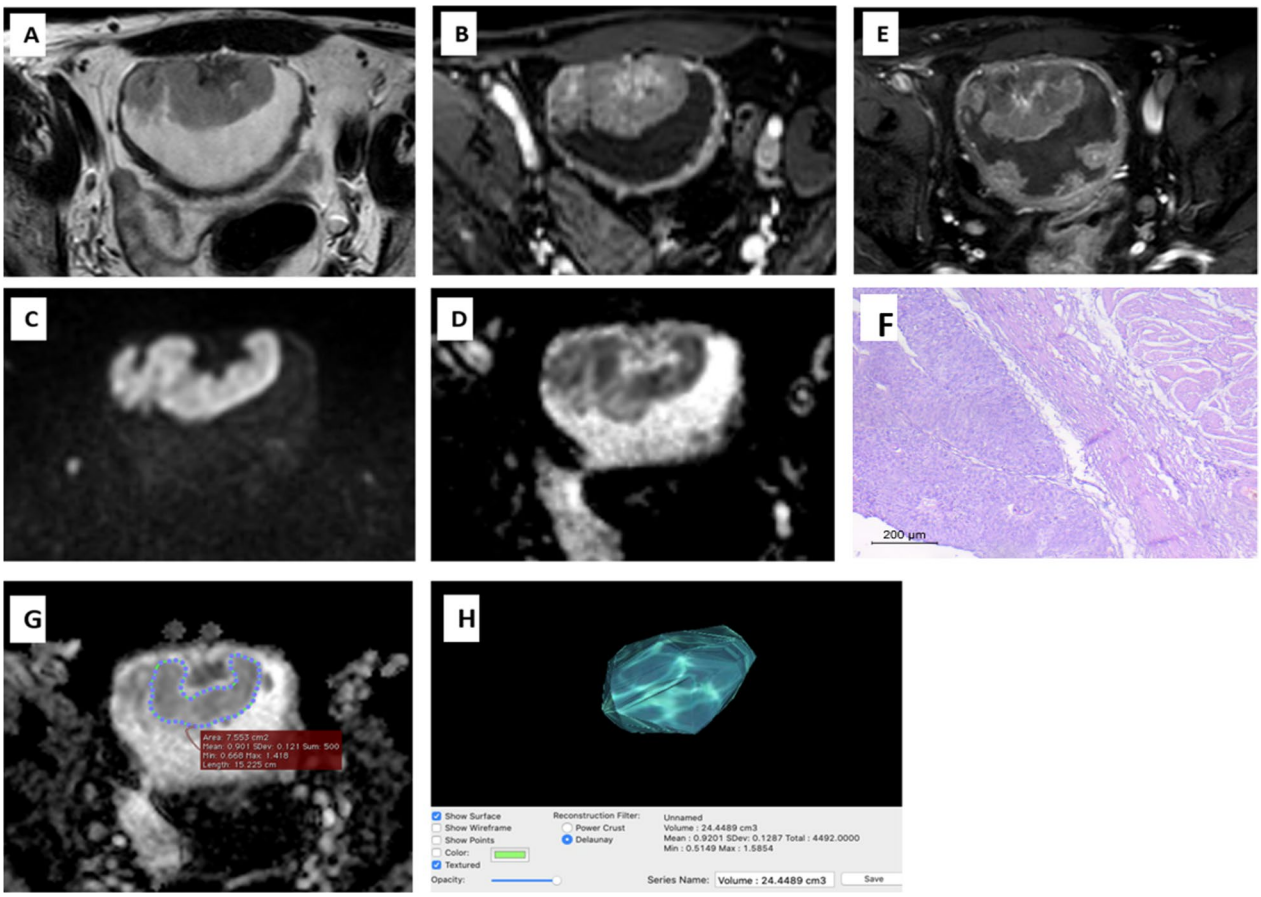


**Fig. 4** A low-grade NMIBC. There are multiple papillary lesions with stalk. Index lesion TCL > 3 cm, 24.4 $cm^3$ in volume, no distal ureteric backpressure, the minimum ADC by selected ROI $0.66 \times 10^{-3}$ $mm^2/s$ and final VI RADS score of 2. **A** Axial T2WI FSE, **B** axial T1WI fat suppression post-contrast, **C** axial DWI at b-value 1000, **D** axial ADC map, **E** axial T1 fat suppression post-contrast showing other lesions, **F** histopathological image showing low-grade non-muscle invasive TCC (100X), **G** tumor segmentation of the index lesion excluding the stalk, **H** calculation of the volumetric values

### Proposed features combinations and their validation

Combining the three variables (final VI RADS score, minimum ADC by ROI and multiplicity) that independently affect muscle invasion on the multivariate regression model did not achieve a higher AUC on ROC curve analysis than the final VI RADS score alone (0.838 compared to 0.895, respectively) while combining only the final VI RADS score and the minimum ADC by ROI had a higher AUC of 0.915. Moreover, when all the six variables analyzed by the univariate regression were combined, this provided the best AUC (0.944) as illustrated in Fig. 6.

## Discussion

MRI examination of bladder cancer to determine the local extension is gaining much attention being a noninvasive procedure with high diagnostic accuracy. Moreover, continuous advances in equipment and imaging techniques have allowed better resolution delineating the anatomical details and developed good imaging markers to predict tumor tissue characteristics. We carried out our study on a 3-T device to attain the best available resolution, and we studied the relation between different imaging variables and the state of muscle invasion.

Bladder cancer is subjected to the field effect, so multifocality is a well-recognized feature noticed in 56.3% of our patients. It has a prognostic value in predicting recurrence and progression [16]. We have noticed this feature in NMIBC cases (75.6%) more than in MIBC (35.9%) to a significant level. It was previously included in a clinicopathological model to predict tumor stage in the pre-cystectomy setting [17]. Nevertheless, a previous study by Wang et al. [18] did not show statistical significance for the multiplicity compared between NMIBC and MIBC.

The most commonly involved bladder region with BC is the lateral walls followed by the trigone [9, 19], as they were involved in 82.5% of all the cases while the trigone was affected in (73.7%). However, differences in regional

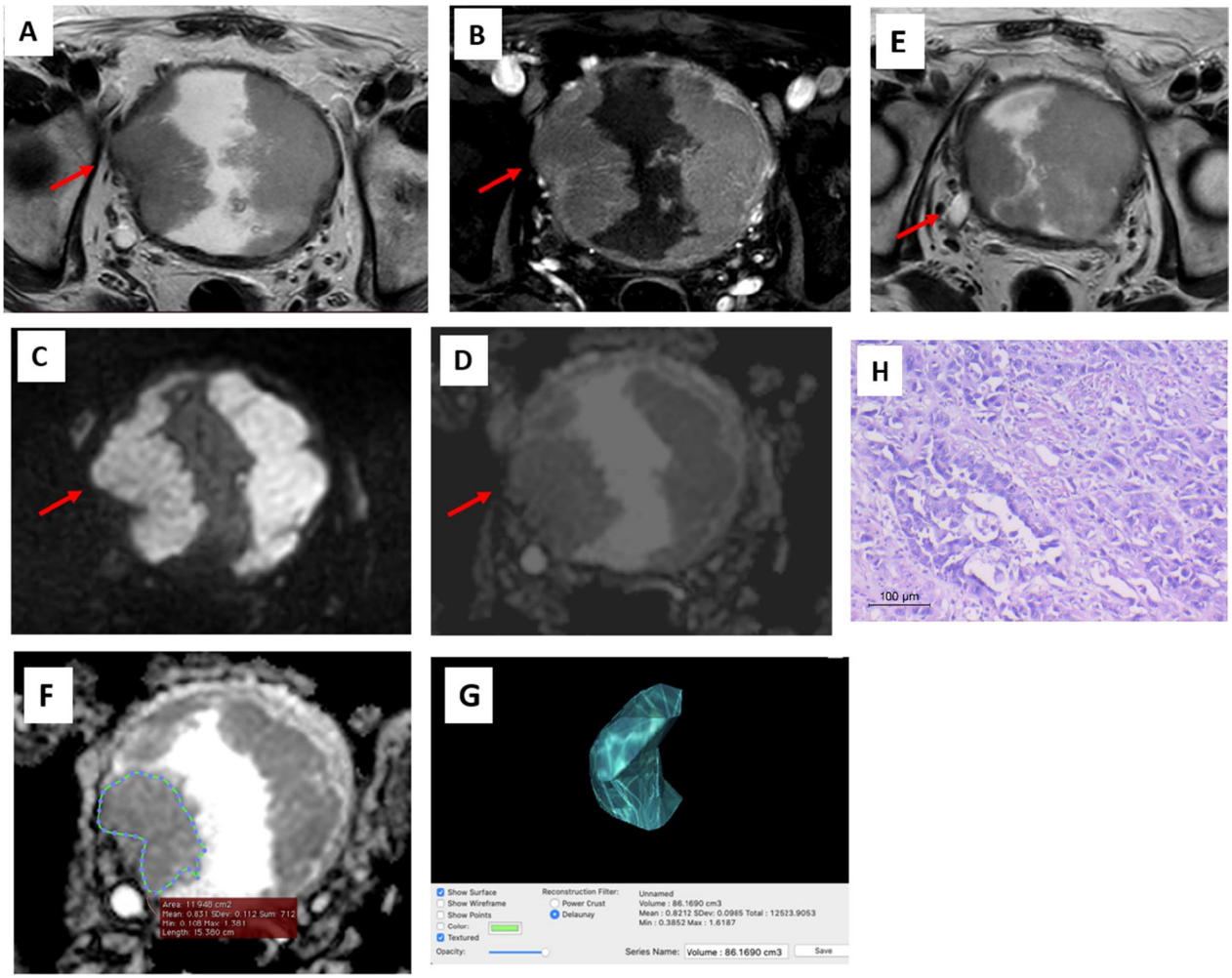


**Fig. 5** A high-grade MIBC. There are multiple lesions. The index lesion seen papillary with thickened inner layer, TCL > 3 cm, 86.17 $cm^3$ in volume, with right distal ureteric backpressure, the minimum ADC by selected ROI $0.4 \times 10^{-3}$ $mm^2/s$ and the final VI RADS score 4. **A** Axial T2WI FSE, **B** axial T1WI fat suppression post-contrast, **C** axial DWI at b-value 1000 and **D** axial ADC map all with red arrows pointing to focal mural invasion by tumor tissue, **E** distal right ureter dilated, **F** tumor segmentation at one slice, **G** calculation of the volumetric values. **H** High-power histopathological image showing high-grade urothelial carcinoma invading the lamina propria (200X)

distribution did not significantly differ between NMIBC and MIBC in the presenting study except for the VUJ involvement (67.5% of all cases) which was significantly involved in MIBC (79.5%) more than NMIBC (56.1%). Previous research described advanced stage, more common nodal involvement and poorer prognosis for lesions at bladder neck and trigone [19, 20] still with no statistical difference between different states of muscle invasion [9].

Distal ureteric backpressure changes seen in 45% of our cases showed statistically significant higher occurrence with MIBC (64.1%) than in NMIBC (26.8%). Hydronephrosis which is the result of ureteric backpressure was similarly proved as a predictor for muscle invasion in the study of Bicchetti et al. [21].

As regards the shape, 70% of the examined lesions were papillary while 30% were sessile. Most of our NMIBC lesions were papillary (90.2%) with statistically significant differences compared to MIBC tumors which were more sessile (51.3%). Non-papillary shape of the bladder tumor showed to be a predictor for progression as compared to the papillary morphology [22]. Another study as well showed that sessile tumors carry a higher risk of muscle invasion [11]. It was also noted that the papillary shape of the tumor was more commonly reported for lesions with lower VI RADS score compared to the sessile morphology in the studies performed by Gupta et al. [6] and Sakamoto et al. [23].

The MIBC lesions had significantly larger mean volume ($2.60 \pm 1.33$ $cm^3$) and TCL (87.2% were above 3 cm) than

**Table 1** Categorical imaging variables showing statistically significant differences between NMIBC and MIBC

| Categorical variables with statistically significant differences | State of muscle invasion | | | | $\chi^2$ | *p* |
|---|---|---|---|---|---|---|
| | NMI (*n* = 41) | | MI (*n* = 39) | | | |
| | No | % | No | % | | |
| **Multiple lesions** | 31 | 75.6 | 14 | 35.9 | 12.809 | < 0.001* |
| **Shape** | | | | | | |
| Papillary | 37 | 90.2 | 19 | 48.7 | 16.413 | < 0.001* |
| Sessile | 4 | 9.8 | 20 | 51.3 | | |
| **Tumor–wall contact length (cm)** | | | | | | |
| ≤ 3 | 25 | 61.0 | 5 | 12.8 | 19.776 | < 0.001* |
| > 3 | 16 | 39.0 | 34 | 87.2 | | |
| **Distal ureteric backpressure** | 11 | 26.8 | 25 | 64.1 | 11.2196 | 0.001* |
| **VUJ involvement** | 23 | 68.3 | 31 | 79.5 | 4.894 | 0.025* |
| **Fibrovascular stalk** | | | | | | |
| Absent | 17 | 41 | 30 | 76.9 | 10.370 | 0.001* |
| Present | 24 | 58.5 | 9 | 23.1 | | |
| Central (inchworm sign) | 12 | 50 | 0 | 0 | 15.985 | < 0.001* |
| Eccentric/distorted | 12 | 50 | 9 | 100 | | |
| **VI RADS SC score** | | | | | | |
| ≤ 3 | 34 | 82.9 | 4 | 10.3 | 42.327 | < 0.001* |
| > 3 | 7 | 17.1 | 35 | 89.7 | | |
| **VI RADS DW score** | | | | | | |
| ≤ 3 | 34 | 82.9 | 4 | 10.3 | 42.327 | < 0.001* |
| > 3 | 7 | 17.1 | 35 | 89.7 | | |
| **VI RADS CE score** | | | | | | |
| ≤ 3 | 33 | 80.5 | 4 | 10.3 | 39.658 | < 0.001* |
| > 3 | 8 | 19.5 | 35 | 89.7 | | |
| **VI RADS final score** | | | | | | |
| ≤ 3 | 33 | 80.5 | 4 | 10.3 | 39.658 | < 0.001* |
| > 3 | 8 | 19.5 | 35 | 89.7 | | |

*NMI* non-muscle invasive, *MI* muscle invasive, *ADC* apparent diffusion coefficient, *VUJ* vesicoureteric junction, $\chi^2$ Chi-square test, **p* value statistically significant at < 0.05

**Table 2** Numeric variables showing statistically significant differences between NMIBC and MIBC

| Numeric variables | State of muscle invasion | | *U* | *p* |
|---|---|---|---|---|
| | NMI (*n* = 41) | MI (*n* = 39) | | |
| **Index tumor volume** ($cm^3$) | 2.15 ± 1.22 | 2.60 ± 1.33 | 579.0 | 0.034 |
| **ADC values** ($\times 10^{-3} mm^2/s$) | | | | |
| Mean ADC for 3 ROIs | 0.87 ± 0.16 | 0.71 ± 0.12 | 350 | < 0.001* |
| Mean ADC for whole tumor volume | 0.93 ± 0.15 | 0.75 ± 0.13 | 268 | < 0.001* |
| Minimum ADC by a selected ROI | 0.67 ± 0.17 | 0.48 ± 0.10 | 229 | < 0.001* |
| Minimum ADC for whole tumor volume | 0.48 ± 0.26 | 0.22 ± 0.16 | 324 | < 0.001* |

*NMI* non-muscle invasive, *MI* muscle invasive, *ADC* apparent diffusion coefficient, *U* Mann–Whitney test, **p* value: statistically significant at < 0.05

NMIBC lesions. Wang et al. and Ahn et al. too proved significantly larger TCL in MIBC than NMIBC [11, 24].

The fibrovascular stalk (seen in 41.3% of our cases) is a known variable that has been correlated with NMIBC; nevertheless, some papers discussed that the shape of the stalk whether central or distorted can increase the accuracy of this variable as some of the MIBC showed a stalk, but it was usually distorted. In general, the stalk

**Table 3** Diagnostic performance for mean and minimum ADC values by ROI and volume methods to predict muscle invasion

| ADC values | AUC | *P* | Cutoff # | Sensitivity | Specificity | PPV | NPV |
|---|---|---|---|---|---|---|---|
| Mean ADC for 3 ROIs | 0.781 | < 0.001* | ≤ 0.76# | 76.92 | 75.61 | 75.0 | 77.5 |
| Mean ADC for whole tumor volume | 0.834 | < 0.001* | ≤ 0.88# | 92.31 | 63.41 | 70.6 | 89.7 |
| Minimum ADC single ROI | 0.857 | < 0.001* | ≤ 0.62# | 97.44 | 58.54 | 69.1 | 96.0 |
| Minimum ADC for whole tumor volume | 0.799 | < 0.001* | ≤ 0.37# | 84.62 | 65.85 | 70.2 | 81.8 |

*AUC* area under a curve, *p* value probability value, *NPV* negative predictive value, *PPV* positive predictive value, *Statistically significant at $p \leq 0.05$ #: Cutoff for Youden index

**Table 4** Categorical variables showing NO statistically significant differences between NMIBC and MIBC

| Categorical variables with NO statistically significant differences | State of muscle invasion | | | | $\chi^2$ | *p* |
|---|---|---|---|---|---|---|
| | NMI (*n* = 41) | | MI (*n* = 39) | | | |
| | No | % | No | % | | |
| Trigonal affection | 28 | 68.3 | 31 | 79.5 | 1.294 | 0.225 |
| Bladder neck | 21 | 51.2 | 24 | 61.5 | 0.865 | 0.352 |
| Urethral extension | 10 | 24.4 | 10 | 25.6 | 0.017 | 0.897 |
| Posterior wall | 25 | 61.0 | 25 | 64.1 | 0.083 | 0.773 |
| lateral walls | 32 | 78.0 | 34 | 87.2 | 1.154 | 0.283 |
| Anterior wall | 19 | 46.3 | 19 | 48.7 | 0.045 | 0.832 |
| Dome and superior wall | 16 | 39.0 | 15 | 38.5 | 0.003 | 0.959 |
| Desmoplastic reaction | 4 | 9.8 | 8 | 20.5 | 1.814 | 0.178 |

*NMI* non-muscle invasive, *MI* muscle invasive, $\chi^2$ Chi-square test, *p* value statistically significant at < 0.05

**Table 5** Univariate and multivariate logistic regression analysis for the imaging parameters affecting muscle invasion state

| Imaging variable affecting muscle invasion | Univariate | | #Multivariate | |
|---|---|---|---|---|
| | *p* | OR (95% CI) | *p* | OR (95% CI) |
| Final VI RADS score ©(≤ 3 vs. > 3) | < 0.001* | 36.094 (9.926–131.254) | 0.030* | 6.702 (1.207–37.215) |
| Index tumor TCL © (≤ 3 vs. > 3 cm) | < 0.001* | 10.625 (3.435–32.864) | 0.170 | 4.530 (0.524–39.135) |
| Index tumor volume ($cm^3$) (n) | 0.221 | 1.005 (0.997–1.014) | | |
| Shape© (Papillary vs Sessile) | < 0.001* | 9.737 (2.910–32.576) | 0.186 | 3.234 (0.568–18.425) |
| Minimum ADC single ROI ($mm^2/s$) (n) | < 0.001* | 0.988 (0.982–0.994) | 0.020* | 0.991 (0.983–0.999) |
| Distal ureter backpressure© | 0.001* | 4.870 (1.881–12.611) | 0.918 | 0.915 (0.167–4.995) |
| Multiple lesions© | 0.001* | 0.181 (0.069–0.475) | 0.024* | 0.133 (0.023–0.770) |

*OR* odd's ratio, *CI* confidence interval, *TCL* tumor–wall contact length

# All variables with $p < 0.05$ were included in the multivariate analysis

*Statistically significant at $p \leq 0.05$, (*C*) category, (n) numeric

was significantly more present in the NMIBC (58.5%) compared to the MIBC (23.1%), but none of the stalks seen in our MIBC cases was central while the NMIBC stalks were equally distributed between being central or eccentric. So conclusively from our study, a central stalk was a better criterion to correlate with NMIBC than the stalk per se that can be also present in MIBC but in a distorted shape. Razik et al. [25] also found that the central stalk was more common in NMIBC and the distorted stalk in MIBC, but none of their NMIBC cases had a distorted stalk.

The desmoplastic reaction with mural retraction was present in 15% of our cases and did not differ significantly in its distribution between NMIBC and MI. It was described that mural retraction is an indirect sign of T2b lesions [26]; however, this neither matched our results nor the results of Wang et al. [24] on 2021, who

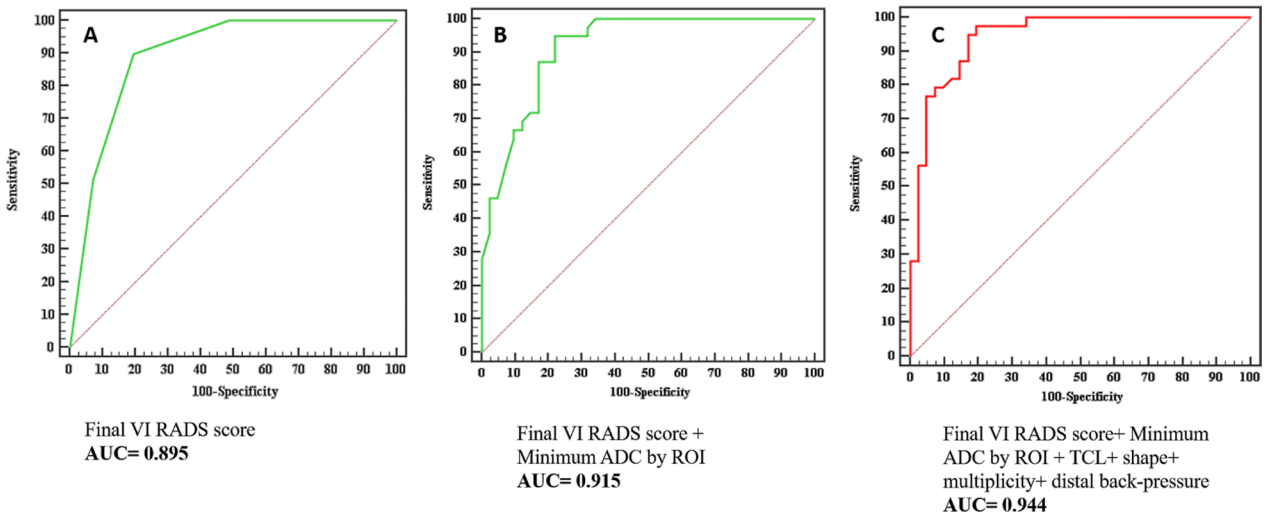


**Fig. 6** ROC curve analyses of different combinations to predict muscle invasion in comparison with VI RADS score alone

also did not find correlation between the state of muscle invasion and mural retraction.

When studying the distribution of our cases in the VI RADS score, only 5% were reported as VI RADS 1 while the higher scores had a range from 18 to 28.8% of the cases in all categories. We considered score (> 3) as a cutoff for muscle invasion, so all categories (SC, DW and CE) as well as the final score were on statistical basis of significant difference between NMIBC and MIBC. This was also proved by ROC curve analysis that showed AUCs ranging from 0.895 to 0.905 with the largest being for the DW category while the sensitivity, specificity, PPV and NPV were nearly the same for all categories and for the final score (89.74%, 80.49–82.93, 81.4–83.33 and 89.19–89.47%, respectively). This goes conjointly with the recommendations of the original VI RADS paper by Panebianco in 2018 to consider the DW as the main sequence to determine the state of muscle invasion [10]. A recently published meta-analysis of previous studies validating the VI RADS score at the cutoff (≥ 3) showed a sensitivity ranging from 77 to 100% and specificity of 50–100% while their own prospective study achieved at the same cutoff a sensitivity, specificity, PPV and NPV of 94.44%, 87.5%, 87.17% and 94.59%, respectively [6].

Variations in the reported ADC values, whether mean or minimum, and in the methods of their measurement are present, so we studied the mean and the minimum ADC values and we calculated them by the ROI and the volumetric methods. The reported values were not the same for both methods, but all of them showed considerable differences in their averages between NMIBC and MIBC. On ROC curve analysis, we obtained the highest AUC for predicting the muscle invasion (0.857) for the minimum ADC value measured by the ROI method. A lower ADC value was also significantly associated with muscle invasion ($p < 0.01$, AUC 0.79) in the study performed by Sakamoto et al. [23], but they measured the mean ADC value only. A meta-analysis was also recently published emphasizing the role of ADC as a biomarker for muscle invasion and high-grade BC [27]. The minimum ADC value was also preferred over the mean values in other organs [14, 28].

A logistic regression model was used to detect the imaging variables having the highest influence on muscle invasion prediction. For statistical consideration, VUJ affection and distal ureteric involvement could not be included together as they are closely related and affect each other, so we only included the distal ureteric backpressure changes. Similarly, we could not include all the measured ADC values, so we had chosen the one with the highest AUC on ROC curve analysis (minimum ADC value with ROI method). The tumor volume was not further incorporated in the multivariate analysis as it proved not to have significance on the univariate analysis ($p$ value was 0.221). The presence of the fibrovascular stalk was already evaluated among the VI RADS score and even the shape of the stalk could not be used as none of the MIBC showed a central stalk. Consequently, the multivariate analysis studied six imaging variables: multiplicity, shape, TCL, distal ureteric backpressure, VI RADS final score and minimum ADC value, resulting in having the multiplicity of the lesions, the final VI RADS score (≤ 3 or > 3) and the minimum ADC value by single ROI as the variables that can independently predict muscle invasion.

A previous study had evaluated the VI RADS score with other radiological variables on a multivariate regression model resulted in having the final VI RADS score, presence of hydronephrosis (backpressure changes) and tumor size as the independent predictors of muscle invasion, but they did not incorporate the ADC value in their analysis [21].

We validated our regression model by ROC curve analysis where the combination of the resultant three variables from the multivariate regression did not show a higher AUC than the VI RADS score alone, in contrast to the combination of the final VI RADS score and minimum ADC by ROI only which showed an AUC higher than either of them alone. On top of that was the combination of all the significant six variables from the univariate regression, showing the best AUC (0.944). Previous studies tried to combine other variables with the VI RADS score to improve its performance and to include quantitative parameters as well. A study performed by Ahn et al. [11] who evaluated the VI RADS score along with different radiological parameters concluded that the VI RADS and the TCL were the two independent variables having significant association with the state of muscle invasion and they may supplement each other to improve prediction. Additionally, Wang et al. proposed a paradigm based on the VI RADS score and TCL to raise the specificity of VI RADS-3 score in predicting muscle invasion [24]. Also Sakamoto et al. [23] studied the effect of combining the standardized mean ADC value to the bi-parametric VI RADS where the AUC was raised from 0.86 to 0.94 and Li et al. [29] as well concluded that combining volumetric ADC histogram parameters to the VI RADS score can enhance its accuracy.

Limitations of our study were the relatively small sample size. External validation was not attempted in our study which is needed on a wider scale to stand on the statistical weight of each parameter in our MR imaging features combination in increasing the diagnostic performance of the VI RADS. Also performing the study on different devices can further allow generalizing these results in order to justify their future incorporation into the VI RADS.

## Conclusions

The well-known high diagnostic accuracy of the VI RADS score can even be improved by simultaneous evaluation of the minimum ADC value by ROI together with tumor multiplicity, shape, TCL and distal ureteric backpressure changes. This achieves the highest possible diagnostic performance on 3-T MRI to predict muscle invasion in bladder cancer.

### Abbreviations

| | |
|---|---|
| VI RADS | Vesical imaging reporting and data system |
| MRI | Magnetic resonance imaging |
| MIBC | Muscle invasive bladder cancer |
| NMIBC | Non-muscle invasive bladder cancer |
| ADC | Apparent diffusion coefficient |
| AUC | Area under the curve |
| ROC | Receiver observer characteristics |
| VUJ | Vesicoureteric junction |
| TCL | Tumor–wall contact length |
| ROI | Region of interest |
| 3-T | 3-Tesla |
| DW | Diffusion-weighted |
| CE | Contrast-enhanced |
| TURBT | Transurethral resection of bladder tumor |
| nac VI RADS | Neoadjuvant chemotherapy VI RADS |
| SC | Structural category |
| DICOM | Digital imaging and communications in medicine |
| re-TURBT | Repeated TURBT |
| TNM | Tumor node metastasis |
| AJCC | American Joint Committee on Cancer |
| IQR | Inter-quartile range |

### Acknowledgements

Not applicable.

### Author contributions

The study's conception and design were settled down by all authors and they all were involved in the writing process and provided feedback on the initial drafts of the paper. AAR and MEE reported the studies. Material preparation, data collection and analysis were done by NEE, OEE and SE. All authors read and approved the final manuscript.

### Funding

This research received no specific grant from any funding agency in the public, commercial or not-for-profit sectors.

### Availability of data and materials

The datasets used and/or analyzed during the current study are available from the corresponding author on reasonable request.

## Declarations

### Ethics approval and consent to participate

Approval was obtained for this prospective study from the institutional review board and the Research Ethics Committee of our University Hospital and informed consent was obtained from the enrolled participants. All study procedures have been carried out adhering to the tenets of the Declaration of Helsinki regarding research involving human subjects.

### Consent for publication

Not applicable. There are no individual person's data provided in this manuscript, and images from MRI are anonymized.

### Competing interests

The authors declare that they have no competing interests.

Received: 4 October 2023 Accepted: 23 December 2023
Published online: 25 January 2024

### References

1. Sung H, Ferlay J, Siegel RL, Laversanne M, Soerjomataram I, Jemal A et al (2021) Global cancer statistics 2020: GLOBOCAN estimates of incidence and mortality worldwide for 36 cancers in 185 countries. CA Cancer J Clin 71(3):209–249

2. Blaveri E, Simko JP, Korkola JE, Brewer JL, Baehner F, Mehta K et al (2005) Bladder cancer outcome and subtype classification by gene expression. Clin Cancer Res 11(11):4044–4055
3. Jobczyk M, Stawiski K, Fendler W, Różański W (2020) Validation of EORTC, CUETO, and EAU risk stratification in prediction of recurrence, progression, and death of patients with initially non-muscle-invasive bladder cancer (NMIBC): a cohort analysis. Cancer Med 9(11):4014–4025
4. Woo S, Suh CH, Kim SY, Cho JY, Kim SH (2017) Diagnostic performance of MRI for prediction of muscle-invasiveness of bladder cancer: a systematic review and meta-analysis. Eur J Radiol 95:46–55
5. Abouelkheir RT, Abdelhamid A, Abou El-Ghar M, El-Diasty T (2021) Imaging of bladder cancer: standard applications and future trends. Medicina 57(3):220
6. Gupta P, Sarangi SS, Singh M, Pandey H, Choudhary GR, Madduri VKS et al (2023) To determine correlation between VIRADS scoring and pathological staging in bladder cancer: a prospective study and review of literature. Urologia 90(3):476–481. https://doi.org/10.1177/03915603231151738
7. Del Giudice F, Flammia RS, Pecoraro M, Moschini M, D'Andrea D, Messina E et al (2022) The accuracy of Vesical Imaging-Reporting and Data System (VI-RADS): an updated comprehensive multi-institutional, multi-readers systematic review and meta-analysis from diagnostic evidence into future clinical recommendations. World J Urol 40(7):1617–1628
8. Pecoraro M, Del Giudice F, Magliocca F, Simone G, Flammia S, Leonardo C et al (2022) Vesical Imaging-Reporting and Data System (VI-RADS) for assessment of response to systemic therapy for bladder cancer: preliminary report. Abdom Radiol 47(2):763–770
9. Panebianco V, Pecoraro M, Del Giudice F, Takeuchi M, Muglia VF, Messina E et al (2022) VI-RADS for bladder cancer: current applications and future developments. J Magn Reson Imaging 55(1):23–36
10. Panebianco V, Narumi Y, Altun E, Bochner BH, Efstathiou JA, Hafeez S et al (2018) Multiparametric magnetic resonance imaging for bladder cancer: development of VI-RADS (Vesical Imaging-Reporting And Data System). Eur Urol 74(3):294–306
11. Ahn H, Hwang SI, Lee HJ, Choe G, Oh JJ, Jeong SJ et al (2021) Quantitation of bladder cancer for the prediction of muscle layer invasion as a complement to the vesical imaging-reporting and data system. Eur Radiol 31:1656–1666
12. Li Q, Cao B, Tan Q, Liu K, Jiang S, Zhou J (2021) Prediction of muscle invasion of bladder cancer: a comparison between DKI and conventional DWI. Eur J Radiol 136:109522
13. Kobayashi S, Koga F, Yoshida S, Masuda H, Ishii C, Tanaka H et al (2011) Diagnostic performance of diffusion-weighted magnetic resonance imaging in bladder cancer: potential utility of apparent diffusion coefficient values as a biomarker to predict clinical aggressiveness. Eur Radiol 21:2178–2186
14. Fan C, Sun K, Min X, Cai W, Lv W, Ma X et al (2022) Discriminating malignant from benign testicular masses using machine-learning based radiomics signature of appearance diffusion coefficient maps: comparing with conventional mean and minimum ADC values. Eur J Radiol 148:110158
15. Sufana Iancu A, Colin P, Puech P, Villers A, Ouzzane A, Fantoni J et al (2013) Significance of ADC value for detection and characterization of urothelial carcinoma of upper urinary tract using diffusion-weighted MRI. World J Urol 31:13–19
16. van Rhijn BW, Hentschel AE, Bründl J, Compérat EM, Hernández V, Čapoun O et al (2021) Prognostic value of the WHO1973 and WHO2004/2016 classification systems for grade in primary Ta/T1 non–muscle-invasive bladder cancer: a multicenter European Association of Urology Non-muscle-invasive Bladder Cancer Guidelines Panel study. Eur Urol Oncol 4(2):182–191
17. Ahmadi H, Mitra AP, Abdelsayed GA, Cai J, Djaladat H, Bruins HM et al (2013) Principal component analysis based pre-cystectomy model to predict pathological stage in patients with clinical organ-confined bladder cancer. BJU Int 111(4b):E167–E172
18. Cai Q, Wen Z, Huang Y, Li M, Ouyang L, Ling J et al (2021) Investigation of synthetic magnetic resonance imaging applied in the evaluation of the tumor grade of bladder cancer. J Magn Reson Imaging 54(6):1989–1997
19. Weiner AB, Desai AS, Meeks JJ (2019) Tumor location may predict adverse pathology and survival following definitive treatment for bladder cancer: a national cohort study. Eur Urol Oncol 2(3):304–310
20. Xiao G-Q, Rashid H (2015) Bladder neck urothelial carcinoma: a urinary bladder subsite carcinoma with distinct clinicopathology. Int J Surg Pathol 23(7):517–523
21. Bicchetti M, Simone G, Giannarini G, Girometti R, Briganti A, Brunocilla E et al (2022) A novel pathway to detect muscle-invasive bladder cancer based on integrated clinical features and VI-RADS score on MRI: results of a prospective multicenter study. Radiol Med 127(8):881–890
22. Park J, Song C, Hong JH, Park B-H, Cho YM, Kim C-S et al (2009) Prognostic significance of non-papillary tumor morphology as a predictor of cancer progression and survival in patients with primary T1G3 bladder cancer. World J Urol 27:277–283
23. Sakamoto K, Ito M, Ikuta S, Nakanishi Y, Kataoka M, Takemura K et al (2020) Detection of muscle-invasive bladder cancer on biparametric MRI using vesical imaging-reporting and data system and apparent diffusion coefficient values (VI-RADS/ADC). Bladder Cancer 6(2):161–169
24. Wang X, Tu N, Sun F, Wen Z, Lan X, Lei Y et al (2021) Detecting muscle invasion of bladder cancer using a proposed magnetic resonance imaging strategy. J Magn Reson Imaging 54(4):1212–1221
25. Razik A, Das CJ, Sharma S, Seth A, Srivastava DN, Mathur S et al (2018) Diagnostic performance of diffusion-weighted MR imaging at 3.0 T in predicting muscle invasion in urinary bladder cancer: utility of evaluating the morphology of the reactive tumor stalk. Abdom Radiol 43:2431–2441
26. Lee CH, Tan CH, Faria SdC, Kundra V (2017) Role of imaging in the local staging of urothelial carcinoma of the bladder. Am J Roentgenol 208(6):1193–1205
27. Kobayashi S, Takemura K, Koga F (2022) Apparent diffusion coefficient value as a biomarker for detecting muscle-invasive and high-grade bladder cancer: a systematic review. Appl Sci 12(3):1278
28. Bickel H, Pinker K, Polanec S, Magometschnigg H, Wengert G, Spick C et al (2017) Diffusion-weighted imaging of breast lesions: region-of-interest placement and different ADC parameters influence apparent diffusion coefficient values. Eur Radiol 27:1883–1892
29. Li S, Liang P, Wang Y, Feng C, Shen Y, Hu X et al (2021) Combining volumetric apparent diffusion coefficient histogram analysis with vesical imaging reporting and data system to predict the muscle invasion of bladder cancer. Abdom Radiol 46(9):4301–4310


## Publisher's Note